

## Molecular arrangement in water: random but not quite

This article has been downloaded from IOPscience. Please scroll down to see the full text article.

2012 J. Phys.: Condens. Matter 24 155102

(<http://iopscience.iop.org/0953-8984/24/15/155102>)

View [the table of contents for this issue](#), or go to the [journal homepage](#) for more

### Download details:

IP Address: 141.209.164.164

The article was downloaded on 16/03/2012 at 13:57

Please note that [terms and conditions apply](#).

# Molecular arrangement in water: random but not quite

V Petkov<sup>1</sup>, Y Ren<sup>2</sup> and M Suchomel<sup>2</sup>

<sup>1</sup> Department of Physics, Central Michigan University, Mt. Pleasant, MI 48858, USA

<sup>2</sup> Advanced Photon Source, Argonne National Laboratory, Argonne, IL 60439, USA

E-mail: [petkov@phy.cmich.edu](mailto:petkov@phy.cmich.edu)


Received 25 October 2011, in final form 20 February 2012

Published 15 March 2012

Online at [stacks.iop.org/JPhysCM/24/155102](http://stacks.iop.org/JPhysCM/24/155102)

## Abstract

Water defines life on Earth from the cellular to the terrestrial level. Yet the molecular level arrangement in water is not well understood, posing problems in comprehending its very special chemical, physical and biological properties. Here we present high-resolution x-ray diffraction data for water clearly showing that its molecular arrangement exhibits specific correlations that are consistent with the presence of rings of H<sub>2</sub>O molecules linked together by hydrogen bonds into tetrahedral-like units from a continuous network. This level of molecular arrangement complexity is beyond what a simple ‘two-state’ model of water (Bernal and Fowler 1933 *J. Chem. Phys.* **1** 515–48) could explain. It may not be explained by the recently put forward ‘chains–clusters of completely uncorrelated molecules’ model (Wernet *et al* 2004 *Science* **304** 995–9) either. Rather it indicates that water is homogeneous down to the molecular level where different water molecules form tetrahedral units of different perfection and/or participate in rings of different sizes, thus experiencing different local environments. The local diversity of this tetrahedral network coupled to the flexibility of the hydrogen bonds that hold it together may explain well the rich phase diagram of water and why it responds non-uniformly to external stimuli such as, for example, temperature and pressure.

 Online supplementary data available from [stacks.iop.org/JPhysCM/24/155102/mmedia](http://stacks.iop.org/JPhysCM/24/155102/mmedia)

(Some figures may appear in colour only in the online journal)

## 1. Introduction

Determining the molecular arrangement in water has been the subject of intense research since the time of the first applications of x-ray diffraction (XRD) [1]. Over the years many diffraction datasets, initially mostly x-ray [3, 4] and later on neutron [5–7], have been collected and, together with data from other molecular-arrangement-sensitive techniques such as x-ray absorption, x-ray Raman [2] and infrared [8] spectroscopy, used to assess structural models for water. Experimental [1–7] and modeling [9] studies have firmly established that water molecules are linked together via hydrogen bonds in a way that each molecule has, on average, 4–5 first neighbors but vary on the more distant molecular arrangement. A common point of view is that water is a random network of H<sub>2</sub>O molecules though the exact type of this network has not been clearly identified. Structural models

featuring water as a mixture of two liquids each with its own distinctive molecular arrangement and density [1, 10, 11] or water composed of chains of strongly bonded molecules immersed in clusters of completely uncorrelated molecules have been put forward as well [2, 12].

To obtain a clearer picture of the molecular arrangement in water diffraction data with very good spatial resolution is necessary. Here we report such data obtained by high energy XRD experiments conducted at a third-generation synchrotron source. The choice of x-rays versus neutrons allows us to (i) achieve a better sensitivity to the oxygen-dominated centers of mass of the water molecules and (ii) avoid the reported quantum level structural differences [13] between normal (H<sub>2</sub>O) and heavy (D<sub>2</sub>O) water. The differences come from the fact that deuterium is much heavier than hydrogen and also bonds involving deuterium are somewhat stronger than corresponding bonds

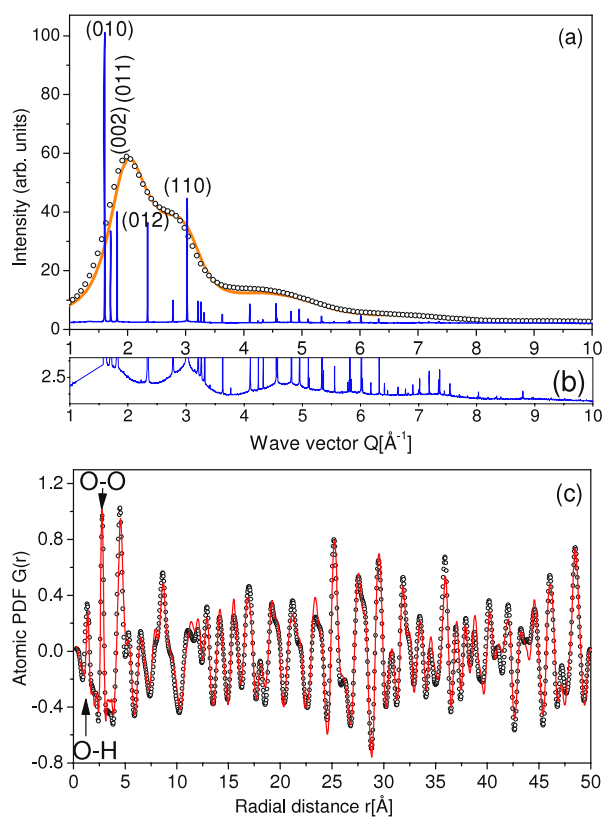


**Figure 1.** Experimental XRD patterns of Ice-Ih (line in blue) and water (dots). The experimental XRD data for water of Hura *et al* [21] are also shown for comparison (line in orange/light gray). Several Bragg peaks in the XRD pattern for Ice-Ih are labeled with their Miller indices (a). Zoom in on the base of the Bragg peaks in the XRD pattern of Ice-Ih, showing the presence of a substantial diffuse scattering (b). Experimental (circles) and model (line in red) atomic PDFs for Ice-Ih. The model PDF is computed from literature data [16, 17] for the average structure of Ice-Ih and so does not account for the presence of local structural distortions. The shortest interatomic distances in Ice-Ih are labeled with the corresponding atomic pairs (c).

involving hydrogen. Indeed those differences are quite substantial and go well beyond the quantum level world since heavy water is much more viscous and has a higher temperature of the density maximum (11.6 °C versus 4 °C) than normal water, reflecting the not exactly equivalent way H<sub>2</sub>O and D<sub>2</sub>O molecules interact together in the liquid. Biochemical and not only physical properties are also affected since life is thriving in normal water while very few species are known to survive in D<sub>2</sub>O.

Molecules in crystalline solids, such as the crystalline forms of frozen water, occupy positions that may be well approximated in terms of three-dimensional (3D) periodic lattices and so act as perfect diffraction gratings when irradiated with x-rays. As a result, their diffraction patterns show a series of sharp Bragg peaks (see figure 1(a)). By analyzing the positions and intensities of those peaks the 3D arrangement of the molecules in the solid crystalline forms of water has already been determined very precisely [14]. Molecules in liquids, however, do not form 3D periodic lattices and so their XRD patterns are very smeared (see

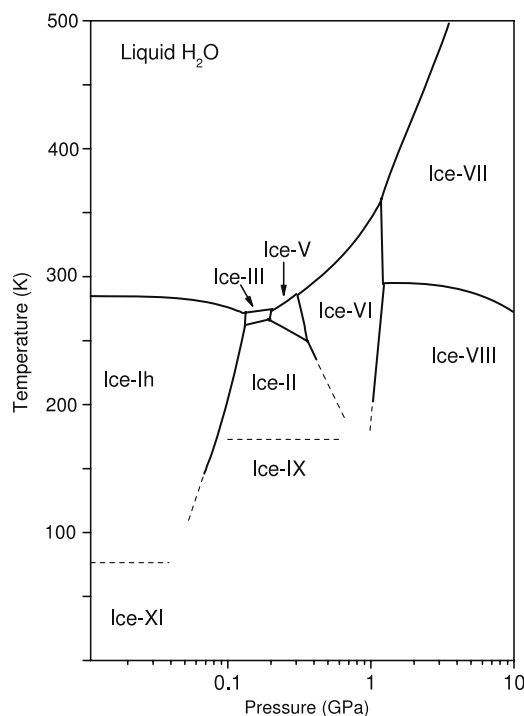


**Figure 2.** Schematic phase diagram of H<sub>2</sub>O in liquid (water) and solid crystalline (ice) state.

figure 1(a)) rendering the traditional, Bragg-peak-based molecular structure determination useless. Here the so-called atomic pair distribution function (PDF) technique is employed which does not consider the smeared diffraction data but their Fourier transform instead [1, 4, 7, 13]. Experimental PDFs peak at distances reflecting frequently occurring inter- and intra-molecular distances while the area under those peaks are proportional to the number of molecules at those distances. This renders PDFs a quantity very well suited for testing and refinement of structural models. To have all PDF details and so the features of the respective molecular arrangement clearly revealed the XRD data has to be collected to high wavevectors,  $q$ , which can be achieved by employing high energy synchrotron radiation x-rays [15].

## 2. Experimental details

To demonstrate the often questioned sensitivity of x-ray-derived PDFs to water we first measured it when frozen (250 K) at normal atmospheric pressure. In such conditions water crystallizes in the so-called Ice-Ih (see figure 2) whose molecular level structure is very well known [14]. The experiments were done at the high-resolution powder diffraction instrument at the beamline 11-BM at the Advanced Photon Source (APS), Argonne National Laboratory. The diffraction data was collected up to wavevectors of 25 Å<sup>-1</sup> using x-rays with a wavelength of 0.4587 Å and a multi-analyzer detection assembly, consisting of 12 independent Si(111) crystal analyzers and LaCl<sub>3</sub> scintillation detectors. The sample, inside a Kapton tube, was measured several times and the patterns averaged out to improve the XRD

data statistics. The total measuring time amounted to 6 h. An empty Kapton tube was measured separately for 1 h. The low- $q$  part of the XRD data from which the scattering due to the Kapton tube has been subtracted out is shown in figure 1(a). The data shows a series of sharp Bragg peaks that may be indexed in terms of a hexagonal lattice of space group  $P6_3/mmc$  [16]. A closer look at the base of the Bragg peaks (see figure 1(b)) reveals a substantial diffuse scattering component, indicating the presence of a substantial local structural disorder. The disorder involves the positioning of the hydrogen atoms about oxygen ones as well as the relative positioning of the neighboring  $H_2O$  molecules with respect to each other [17]. The XRD data was reduced to an atomic PDF using the scattering factors of free hydrogen and oxygen atoms. In the reduction process the inelastic, also known as Compton, scattering had to be removed from the measured XRD intensities since the PDFs are based on their elastic part [4, 18] only. It was done by using the tabulated values of Thijsse (see equation (A2) in [18]) for Compton scattering together with a proper particular crystal analyzer detector set-up attenuation function [19]. The resulted PDF is shown in figure 1(c). Within this free-atom approximation the charge transfer from hydrogen to oxygen in the  $H_2O$  molecules is neglected but then the atomic PDF data can be directly matched against structural models derived from traditional, single-crystal diffraction experiments. As can be seen in figure 1(c) the experimental atomic PDF for Ice-Ih shows a series of well-defined peaks reflecting the presence of a sequence of very well-defined coordination spheres in this crystalline material. All PDF peaks can be very well approximated with a structural model<sup>3</sup> featuring the well-known hexagonal structure of Ice-Ih verifying the excellent sensitivity of x-ray-derived PDFs to materials of high hydrogen content such as water.

XRD data for liquid water inside a thin-walled capillary were obtained at room temperature (295 K) and normal (atmospheric) pressure at the 11-ID-C beamline at the Advanced Photon Source, Argonne National Laboratory up to wavevectors of  $25 \text{ \AA}^{-1}$ . X-rays with a wavelength of  $0.107 \text{ \AA}$  (i.e. with an energy of 115.24 keV) and a large-area detector were employed. Several scans were taken and averaged out to improve the XRD data statistical accuracy. The total measuring time amounted to 12 h. An empty capillary was measured separately for 1 h to evaluate the sample container and environment, air in this case, scattering. To make our XRD data directly comparable to those of previous structural studies of water here we took into account the substantial transfer of charge from hydrogen to oxygen within the water molecules. Following the protocol described in [4, 20–22]

<sup>3</sup> The structure parameters of Ice-Ih resulted from the atomic PDF refinement are as follows: lattice parameters  $a = 4.528 \text{ \AA}$  and  $c = 4.528 \text{ \AA}$ , oxygen position at (0.333, 0.6667, 0.084), and hydrogen positions at (0.3333, 0.6667, 0.17) and (0.51, 0.97, 0.024). The oxygen position is fully occupied while the hydrogen is half occupied. Those parameters are very close to the ones obtained by single-crystal diffraction experiments [16]. The remaining small differences between the experimental and model computed atomic PDFs are due to the fact that the model was constrained to the symmetry of a perfect (space group  $P6_3/mmc$ ) hexagonal lattice and so the presence of local structural disorder in Ice-Ih was not accounted for.

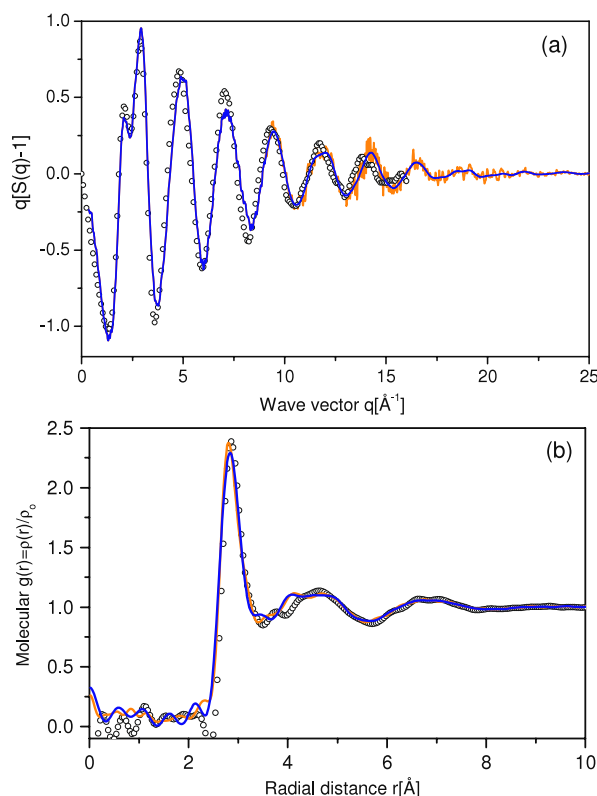


**Figure 3.** Experimental intermolecular structure function for water (line in orange/light gray) and a minimum noise [23] extrapolation to it (line in blue/dark gray). The experimental data of Narten and Levy (circles) [4] are shown as well (a). Intermolecular PDF  $g(r)$  for liquid water (line in orange/light gray) obtained from the present experimental data and the  $g(r)$  of Narten and Levy (circles). Intermolecular PDF for liquid water (line in blue/dark gray) obtained from a portion of the present experimental data extending to wavevectors  $q$  of  $12 \text{ \AA}^{-1}$  only is shown as well. This lower resolution  $g(r)$  shows noticeable termination (with unphysical high-frequency behavior) ripples (e.g. see the region below  $2 \text{ \AA}$ ) and diminished resolution manifested by the loss of sharpness in the PDF's peaks at about  $2.80(1)$  and  $3.5(1) \text{ \AA}$  (b).

we computed the scattering of a single  $H_2O$  molecule, i.e. the scattering due to intra-molecular atomic correlations, and subtracted it from the experimental XRD data. The low- $q$  part of the corrected for intra-molecular and sample container scattering XRD data for water is shown in figure 1(a). They agree quite well with the data of Hura *et al* [21] showing a principal peak at about  $2 \text{ \AA}^{-1}$  with a prominent shoulder at about  $3 \text{ \AA}^{-1}$  followed by a few more, very broad oscillations. The data was reduced to the so-called intermolecular structure function [4, 22] of water shown in figure 3(a). In the reduction process the Compton scattering was evaluated again using the values tabulated in [18]. This time no wavevector-dependent attenuation function [19] was applied since large-area detectors are not x-ray energy-discriminating. The Breit–Dirac recoil factor (see the pre-factor of equation (A2) in [18]), however, had to be adjusted to account for the energy efficiency of the particular area detector used. The respective intermolecular PDF  $g(r) = \rho(r)/\rho_0$ , where  $\rho(r)$  and  $\rho_0$  are the local and average molecular density of

water, respectively, is shown in figure 3(b). The structure function (figure 3(a)) agrees quite well with that obtained by Narten and Levy [4] but extends to much higher wavevectors thanks to the usage of x-rays of much higher energy and brilliance in the present study. Accordingly, the respective molecular PDF is of much improved resolution and lower level of experimental artifacts such as Fourier termination ripples (see figure 3(b)) than all previously obtained x-ray PDFs for water. The PDF shows a first peak positioned at 2.80(1) Å followed by a small hump at about 3.5(1) Å and a clearly split second peak with two components located at 4.1(1) and 4.7(1) Å. A third broad  $g(r)$  peak is seen positioned between 6 and 8 Å. Those characteristic  $g(r)$  features were found very reproducible when checked against possible experimental artifacts with data noise-sensitive analytical procedures [23]. Indeed several x-ray-derived molecular PDFs for water obtained from datasets extending to wavevectors  $q_{\max}$  of at least  $15 \text{ \AA}^{-1}$ , including the early datasets of Narten *et al* [4, 24] and the more recent one of Fu *et al* [22], reveal, though not so clearly as the present data, the characteristic PDF's features listed above. Unfortunately, quite a few PDF datasets currently in use for testing and verifying structural models of water do not show those features clearly mostly due to the low  $q_{\max}$  of the respective experiments and/or to the applying of artificial PDF data smoothing procedures as discussed in [22].

As already well established [4, 7, 20–22] the first PDF peak positioned at 2.80(1) Å reflects the correlations between the immediate neighbor  $\text{H}_2\text{O}$  molecules in water. The distinct PDF features beyond it show the presence of a specific organization of the second and further coordination spheres of those molecules. It is worth noting that, when water is carefully frozen into amorphous ice, the higher-order correlations at approximately 3.5(1) Å, 4.1(1) Å and 4.7(1) Å become even more prominent (see figure 7 in [25]), indicating that, under the particular thermodynamic conditions, they have become even more preferred by the  $\text{H}_2\text{O}$  molecules. Also, a clear evolution of the 3.5 Å PDF feature is observed with water subjected to increased temperature [26, 27] or pressure [28].

### 3. Discussion

To identify the origin of the higher-order molecular correlations in water seen in our high-resolution PDF data we looked at some of water's solid forms that (i) are crystalline and so have their molecular arrangement very precisely determined and (ii) are thermodynamically very close to it and, just like amorphous ice studied in [25], may have inherited some of its specific structural features. Molecular PDFs for such three crystalline forms of water, in particular for Ice-Ih, Ice-II and Ice-III (see figure 2), are shown in figure 4(a). Those were computed from the respective well-known crystal structures [14]. At first, PDFs for infinite Ice-Ih, Ice-II and Ice-III crystals were computed by applying periodic boundary conditions on the unit cells of the respective crystalline lattices. Then each of the coordination spheres of these perfect crystals, i.e. each of the peaks of

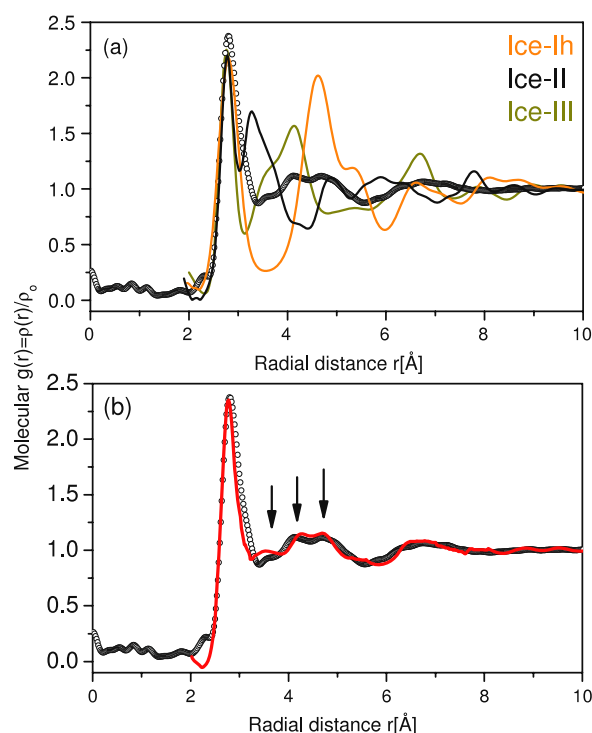


**Figure 4.** Experimental intermolecular PDF for water (symbols). Model PDFs for heavily distorted structures of crystalline Ice-Ih (line in orange/light gray), Ice-II (line in black) and Ice-III (line in dark yellow/gray) are shown as well (a). A model PDF computed (line in red) as a linear combination of the model PDFs of Ice-Ih, Ice-II and Ice-III is seen to reproduce the experimental data reasonably well (b). Arrows mark the positions of higher-order molecular correlations in water that are consistent with the presence of ring-type configurations of a tetrahedral network.

the respective PDFs, was broadened by a convolution with a Gaussian function to take into account the presence of dynamic (i.e. thermal) and static disorder in water. At the same time the computed PDFs  $g(r)$  were multiplied by a rapidly decaying function which is completely flat for distances of about 10 Å beyond which the experimental PDF for water (see figure 3(b)) shows no physical oscillations. Thus computed PDFs (shown in figure 4(a)) represent bulk matter with very well-defined local but no longer range order, i.e. matter with a liquid-type molecular arrangement. In particular, all three PDFs show a very well-defined first peak positioned at about 2.80(1) Å reflecting the presence of tetrahedrally coordinated  $\text{H}_2\text{O}$  molecules in these ices. The tetrahedral units of  $\text{H}_2\text{O}$  molecules in Ice-Ih are quite perfect, in a sense that the bond angles between the molecules forming those units are close to the ideal tetrahedral angle of  $109.5^\circ$  [14]. The molecules are coupled via hydrogen bonds in somewhat buckled hexagonal rings of chair- and boat-type configurations. The two types of rings alternate with each other, forming a relatively open, parallel channel-riddled structure (see figure 5, left) with density ( $0.917 \text{ g cm}^{-3}$ ) less than that of water ( $0.99 \text{ g cm}^{-3}$ ). The correlations between the next-nearest  $\text{H}_2\text{O}$  molecules from those rings are seen as a split second peak, positioned between 4 and 6 Å (see the respective model PDF shown in figure 4(a)). The tetrahedral units of  $\text{H}_2\text{O}$  molecules are more distorted in Ice-II and

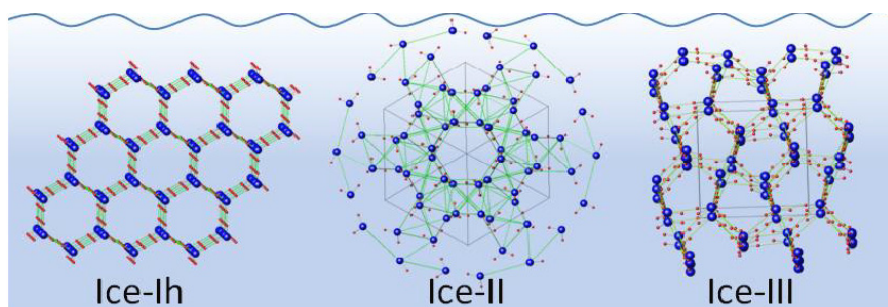


**Figure 5.** Fragments from the molecular arrangement in Ice-Ih (left), Ice-II (middle) and Ice-III (right). In water the fragments would be a part of a continuous tetrahedral network. Oxygen atoms (larger dots) are in dark blue, hydrogen (smaller dots) in red. Green lines connect the first-neighbor oxygen atoms showing the existence of well-defined rings of H<sub>2</sub>O molecules. The distances between molecules from rings sharing a common side extend up to 10–15 Å. It is worth noting that this is the distance usually associated with the spatial extent of the so-called hydration forces [38].

Ice-III. In Ice-II they also form six-membered rings but some of those rings are flattened. In addition, those more distorted units form a more dense structure (see figure 5, middle) where only one-third of the type of open channels seen in Ice-Ih is present. A distinctive feature of the tetrahedral network of Ice-III is the presence of non-flat five-membered rings; seven-membered rings are also present (see figure 5, right). The network structure of Ice-III is also denser than that of Ice-Ih. Furthermore, contrary to the case of Ice-Ih, where all H<sub>2</sub>O molecules have the same type of four, hydrogen-bound immediate neighbors, the H<sub>2</sub>O molecules in Ice-II and Ice-III have two types of near-neighbors. The first type are four, hydrogen-bound immediate neighbors from a five-, six- or seven-membered ring. The second, one or two in number, are neighbors belonging to rings coming very close to the first coordination shell of a given H<sub>2</sub>O molecule that is not associated with those rings by a hydrogen bond. The more closely packed neighborhood of the H<sub>2</sub>O molecules in Ice-II and Ice-III (four hydrogen-bonded plus one or two not-bonded neighbors) renders them denser (by 20–25%) than Ice-Ih and (by 10–15%) water. The more closely packed neighborhood of the H<sub>2</sub>O molecules in Ice-II and Ice-III is seen as a split second PDF peak appearing at distances shorter than 4 Å (see figure 4(a)). As can be seen in figure 4(a) the second coordination spheres of Ice-Ih, Ice-II and Ice-III are very close in position to the distinct 3.5(1), 4.1(1) and 4.7(1) Å features in the experimental molecular PDF of water. Furthermore, a linear combination of the model PDFs for Ice-Ih, Ice-II and Ice-III (60% of that of Ice-Ih and the rest a mixture of those of Ice-II and Ice-III) reproduces quite well the overall shape of the experimental data as can be seen in figure 4(b). The density of this ‘linear combination’ model is also very close to that of water. The thus-constructed model envisages a few distinct types of H<sub>2</sub>O molecule neighborhoods embedded into a medium with no longer than 10 Å in range correlations. It is a simplistic approximation to the real molecular arrangement in water and used here only to identify the possible origin of the fine features in the experimental molecular PDF for water we observed. The model results show that those features may come from the presence of well-defined five-, six- and seven-membered rings from a network of tetrahedrally like connected by hydrogen bonds H<sub>2</sub>O molecules with the

number of the six-membered rings prevailing (60%) over that of the others.

Note that previous studies have also approached the molecular PDF for water with structural models featuring a linear combination of computed PDFs. For example, Robinson *et al* [29] constructed a model featuring a combination of Ice-Ih and Ice-II type bonding. On the other hand, Jhon *et al* [11] suggested a model featuring water as a mixture of Ice-Ih and Ice-III type bonding. We found it impossible to approximate the higher-order molecular correlations in water with a model based on just two of its crystalline modifications. Hall [10] was among the first to suggest that water is separated in two phases of non-interacting molecules. Later on Sopper *et al* [30] suggested a model featuring a combination of a low-density relatively open, hydrogen-bonded tetrahedral structure and a high-density, non-tetrahedral structure with some broken hydrogen bonds. A refined version of this model featuring a mixture of two phases divided by a common hydrogen bond was put forward very recently [31]. Also, Okhulkov *et al* (see figure 8 in [28]) constructed a model featuring a linear combination of computed PDFs for Ice-Ih (50%), Ice-III (22%) and a simple, essentially non-tetrahedral-type Lennard-Jones fluid (28%). We found it unnecessary to include ingredients featuring a different than tetrahedral-type bonding in our structural model. We could have constructed a more refined model by including other types of crystalline ice structures and/or other types of rings, including a fraction of smaller than five (e.g. fourfold) and larger than seven (e.g. eightfold) rings that studies [32, 33] suggest may exist in liquid water. However, we did not do it since we were not after constructing a very complicated model as to reproduce the experimental PDF data in the finest detail. Rather we looked for a model of minimum complexity that is based on well-documented similarities [14] between liquid water and its closest solid forms, particularly aiming at identifying and so verifying the physical origin of the 3.5 Å feature and the split second major peak, i.e. the 4.1 Å and 4.7 Å features, in the molecular PDF of water. Our simplistic approach showed that these higher-order molecular correlations in water can be reasonably well reproduced by a model based on its three thermodynamically closest crystalline modifications:

namely Ice-Ih, Ice-II and Ice-III (see figure 2) that all are tetrahedral-type networks of H<sub>2</sub>O molecules. Note that, had those fine PDF's features been pure experimental artifacts (e.g. noise), such a reasonable agreement (see figure 3(b)) would have been very unlikely to be observed. Here we also have to stress out that the fact that the experimental molecular PDF for water may be approximated by a linear combination of PDFs for three of its solid crystalline forms does not imply that water is a 'mixture' of different phases, each with its distinct structure and density. Such a macroscopic mixture would inevitably show macroscale density fluctuations that have never been detected experimentally in a conclusive way [34]. It merely indicates that, although random, i.e. lacking extended 3D order and periodicity, the arrangement of the H<sub>2</sub>O molecules in liquid water is not completely untidy but shows a preference for specific, ring-type configurations of a type seen in the tetrahedral-type networks of water frozen into crystalline ices (see figure 5).

Tetrahedral-type networks are often seen in condensed matter involving atomic species that interact via directional in character bonds. An archetypical example is silica. It has several crystalline modifications that are 3D ordered networks of corner-sharing Si–O<sub>4</sub> tetrahedra. Silica glass too is a network of such units though the network here is random, again in a sense that it lacks 3D order and periodicity [35]. Yet it has a very characteristic distribution of rings that involve from five to about nine Si–O<sub>4</sub> tetrahedra [36]. The analogy between silica glass and water has been first brought about by Bernal and Fowler back in 1934 [1]. They noticed that both materials have several crystalline modifications and even the ordering of the Si atoms in the  $\beta$ -tridymite crystalline modification of silica is like that of the oxygen atoms in the Ice-Ih crystalline form of water. Furthermore, molten silica exhibits several peculiar anomalies that are similar to the ones observed with liquid water, including a negative temperature expansion, density maximum and a heat capacity minimum [37].

Following Bernal and Fowler's analogy and armed with the results of the present study a model picture for water may be put forward viewing it (i) as a random network of tetrahedral-like units where (ii) the tetrahedral units have various degrees of perfection (e.g. some may be as perfect as in Ice-Ih and others as deformed as in Ice-III) and (iii) are further interconnected via hydrogen bonds in flat or buckled rings (see figure 5), preferably made of six such units. A lesser but definitely not negligible number of smaller (e.g. fivefold) and larger (e.g. sevenfold) rings are present as well. This level of tetrahedral network complexity is beyond what the simple 'two-state' model of water suggested by previous studies [1, 10, 29] could explain. It may not be explained by the recently suggested 'chains–clusters of completely uncorrelated molecules' model [2] either. Rather it features a tetrahedral network that is continuous down to the molecular level where several (flat and buckled, five-, six-, seven-membered, etc) but limited in number types of ring configurations exist as an integral part of the network<sup>4</sup>.

<sup>4</sup> Indeed it would be plausible to assume that the ring distribution in the tetrahedral network of water molecules spans somewhat below

Hydrogen bonds in distorted tetrahedra are weakened [14] and so would be the respective ring fragments from the network. Water molecules from the network that have more closely packed neighborhoods (e.g. Ice-III type-like neighborhood) than others (e.g. Ice-Ih type-like neighborhood) would be more constrained and so would have different vibrational amplitudes. Local probe techniques (e.g. IR and Raman) that are sensitive to the strength of hydrogen bonds and molecular vibrations would single out such parts of the tetrahedral network of water as static and/or dynamic inhomogeneities [2, 8, 38] though, in light of the discussion above, the term 'tetrahedral network local non-uniformities' would be more appropriate. Note that, although present, such non-uniformities are not detected in the random tetrahedral network of silica glass where, thanks to the much greater strength of Si–O bonds, all Si–O<sub>4</sub> units are virtually the same and with the same local environment, hence, the same first coordination number of four. In water the molecules with a more open, Ice-Ih type neighborhood would have a coordination number of four; others that have the Ice-II and III type of environment would have a first coordination number of 5 or 6, bringing the average coordination number to larger than 4. If estimated by integrating the first peak of our molecular PDF to a distance of about 3.3 Å the coordination number comes close to 4.4(2).

The presence of distinct ring-type configurations in the tetrahedral network coupled to the flexibility of its underlying hydrogen bonding [14] may explain well why the pressure–temperature phase diagram of water is so rich in liquid [39], solid crystalline (see figure 2) and solid amorphous states [25, 40]. At given thermodynamic conditions a particular local structural feature (e.g. six-membered buckled rings) may become more favored and evolve further at the expense of others, driving the whole network in a particular phase state (e.g. Ice-Ih). Solute (e.g. drug, protein, etc) molecules may cause a similar effect [41]. Even without a sizable change in the external thermodynamic conditions or adding solutes but just by virtue of the well-known effect of epitaxy the tetrahedral network of water confined in small size volumes, e.g. such as inside carbon nanotubes, may evolve into a particular structural state, e.g. favoring five/seven-membered rings and the respective penta/heptagonal local symmetry [42], that best conforms to its extended environment. A five-membered ring/pentagonal local symmetry favoring structural state has also been observed in water confined in collagen [38]. It may also explain well why water may respond non-uniformly to external stimuli. Competition between the local structural features of the tetrahedral network (e.g. buckled versus flattened rings) and takeovers of some over others (e.g. Ice-II, III type neighborhood taking over the Ice-Ih type with increasing temperature and pressure as manifested by the respective strengthening of the PDF feature at

five- and above seven-membered rings with a further decreasing rate of ring occurrences as in other tetrahedral-type random networks, and as theory [32, 33] predicts. A PDF for a network with such a broader ring size distribution may reproduce the experimental data for water even better than what is shown in figure 4(b).

3.5 Å [26–28]) may give rise to a non-uniform behavior of the network as a whole, leading to the well-known coefficient of thermal expansion, compressibility and other anomalies of water [9, 43].

#### 4. Conclusions

In summary, the results of the present high energy XRD study clearly show the presence of a specific organization beyond the first coordination sphere of the water molecules, in particular the presence of distinct, higher-order molecular correlations at 3.5(1), 4.1(1) and 4.7(1) Å. The organization may be explained in terms of distinct ring-type configurations of a continuous tetrahedral-type network with the number of six-membered rings prevailing over that of smaller (e.g. five-membered) and larger (e.g. seven-membered) ones. Thanks to the flexibility of the underlying hydrogen bonding different water molecules from the network may have different near-neighbor environments by participating in tetrahedral units of different perfection and/or in rings that may approach each other to a different extent. The coexistence of these distinct environments and the relative easiness of reforming them into each other due to hydrogen bonding would definitely affect the properties of water and so should not be neglected. In this respect the present high-resolution PDF data<sup>5</sup> can help refine our view of water, including all theoretical models for water that largely seem to underestimate [44, 45] the higher-order molecular correlations in it.

#### Acknowledgment

Work at APS was supported by the DOE under contract DE-AC02-06CH11357.

#### References

- [1] Bernal J D and Fowler R H 1933 *J. Chem. Phys.* **1** 515–48
- [2] Wernet Ph *et al* 2004 *Science* **304** 995–9
- [3] Morgan J and Warren B E 1938 *J. Chem. Phys.* **6** 666–73
- [4] Narten A H and Levy H A 1971 *J. Chem. Phys.* **55** 2263–9
- [5] Narten A H 1972 *J. Chem. Phys.* **56** 5681–7
- [6] Thiessen W E and Narten A H 1982 *J. Chem. Phys.* **77** 2656–62
- [7] Soper A K 2000 *Chem. Phys.* **258** 121–37
- [8] Fecko C F, Eaves J D, Loparo J J, Tokmakoff A and Geissler P L 2003 *Science* **301** 1698–702
- [9] Paesani F and Voth G A 2009 *J. Phys. Chem.* **113** 5702–19
- [10] Hall L 1947 *Phys. Rev.* **73** 775–81
- [11] Jhon M S, Grosh J, Ree T and Eyring H 1966 *J. Chem. Phys.* **44** 1465–72
- [12] Mishima O and Stanley H E 1998 *Nature* **396** 329–35
- [13] Ball P 2008 *Nature* **452** 291–2
- [14] Soper A K and Benmore C J 2008 *Phys. Rev. Lett.* **101** 065502
- [15] Malenkov G 2009 *J. Phys.: Condens. Matter* **21** 283101
- [16] Petkov V, Billinge S J L, Shastri S D and Himmel B 2000 *Phys. Rev. Lett.* **85** 3436–9
- [17] Goto A, Hondoh T and Mae S 1990 *J. Chem. Phys.* **93** 1412–7
- [18] Kuhs W F and Lehmann M S 1983 *J. Phys. Chem.* **87** 4312
- [19] Nield V M and Whitworth R W 1995 *J. Phys.: Condens. Matter* **7** 8259–71
- [20] Thijsse B J 1984 *J. Appl. Crystallogr.* **17** 61–76
- [21] Ruland W 1964 *Br. J. Appl. Phys.* **15** 1301–7
- [22] Badyal Y S, Saboungi M-L, Price D L, Shastri S D, Haeffner D R and Soper A K 2000 *J. Chem. Phys.* **112** 9206–8
- [23] Hura G, Sorenson J M, Glaeser R M and Head-Gordon T 2000 *J. Chem. Phys.* **113** 9140–8
- [24] Fu L, Bienenstock A and Brennan S 2009 *J. Chem. Phys.* **131** 234702
- [25] Petkov V and Danev R 1998 *J. Appl. Crystallogr.* **31** 609–19
- [26] Narten A H, Danford M D and Levy H A 1967 *Discuss. Faraday Soc.* **43** 93–107
- [27] Narten A H, Venkatesh C G and Rice S A 1976 *J. Chem. Phys.* **64** 1106–21
- [28] Bosio L, Chen S-H and Teixeira J 1983 *Phys. Rev. A* **2** 1468–76
- [29] Huang C, Wikfeldt K T, Nordlund D, Bergmann U, McQueen T, Sellberg J, Pettersson L G M and Nilson A 2011 *Phys. Chem. Chem. Phys.* **13** 19997–20007
- [30] Okhulkov A V, Demianets Yu N and Gorbaty Yu E 1994 *J. Chem. Phys.* **100** 1578–88
- [31] Robinson G W, Cho Ch H and Urquidi J 1999 *J. Phys. Chem.* **111** 698–702
- [32] Soper A K and Ricci M A 2000 *Phys. Rev. Lett.* **84** 2881–4
- [33] Soper A K 2011 *J. Phys. Chem. B* **115** 14014–22
- [34] Matsumoto M 2007 *J. Chem. Phys.* **126** 054503
- [35] Matsumoto M, Baba A and Ohmine I 2007 *J. Chem. Phys.* **127** 134504
- [36] Clark G N I, Hura G, Teixeira J, Soper A K and Head-Gordon T 2010 *Proc. Natl Acad. Sci.* **107** 14003–7
- [37] Zachariasen W H 1932 *J. Am. Chem. Soc.* **54** 3841–51
- [38] Van Ginhoven R M, Jönsson H and Corrales L R 2005 *Phys. Rev. B* **71** 024208
- [39] Shell M S, DeBenedetti P G and Panagiotopoulos A Z 2002 *Phys. Rev. E* **66** 011202
- [40] Walrafen G E and Chu Y-C 2000 *Chem. Phys.* **258** 427–46
- [41] Strässle Th, Saitta A M, Godec Y Le, Hamel G, Klotz S, Loveday J S and Nelmes R J 2006 *Phys. Rev. Lett.* **96** 067801
- [42] Finney J L, Bowron D T, Soper A K, Loerting T, Mayer E and Hallbrucker A 2002 *Phys. Rev. Lett.* **89** 205503
- [43] Soper A K 2000 *Physica B* **276–278** 12–6
- [44] Koga K, Gao G T, Tanaka H and Zeng X C 2001 *Nature* **412** 802–5
- [45] Stanley H E, Buldyrev S V, Franzese G, Giovambattista N and Starr F W 2005 *Phil. Trans. R. Soc. A* **363** 509–23
- [46] Chialvo A A, Yezdimer E, Driesner Th, Cummings P T and Simonson J M 2000 *Chem. Phys.* **258** 109–20
- [47] Soper A K 2007 *J. Phys.: Condens. Matter* **19** 335206

<sup>5</sup> See supplemental material (available at [stacks.iop.org/JPhysCM/24/155102/mmedia](http://stacks.iop.org/JPhysCM/24/155102/mmedia)) for the low- $q$  part of the experimental XRD pattern for water (shown in figure 1(a)), the experimental molecular structure function  $q(S(q) - 1)$  for water and the minimum noise approximation to it (both shown in figure 3(a)), and the experimental molecular PDF  $g(r)$  for water (shown in figures 3(b) and 4).